Thickness-dependent cooperative aging in polycrystalline films of antiferromagnet CoO

Tianyu Ma, Xiang Cheng, Stefan Boettcher, Sergei Urazhdin, and Lydia Novozhilova

Phys. Rev. B **94**, 024422 — Published 18 July 2016

DOI: 10.1103/PhysRevB.94.024422

Thickness-dependent cooperative aging in polycrystalline films of antiferromagnet CoO

Tianyu Ma, Xiang Cheng, Stefan Boettcher, and Sergei Urazhdin
Department of Physics, Emory University, Atlanta, GA 30322

Lydia Novozhilova
Department of Mathematics, Connecticut State University, Danbury, CT 06810

We demonstrate that thin polycrystalline films of antiferromagnet CoO, in bilayers with ferromagnetic Permalloy, exhibit slow power-law aging of their magnetization state. The aging characteristics are remarkably similar to those previously observed in thin epitaxial $Fe_{50}Mn_{50}$ films, indicating that these behaviors are likely generic to ferromagnet/antiferromagnet bilayers. In very thin films, aging is observed over a wide temperature range. In thicker CoO, aging effects become reduced at low temperatures. Aging entirely disappears for large CoO thicknesses. We also investigate the dependence of aging characteristics on temperature and magnetic history. Analysis shows that the observed behaviors are inconsistent with the Neel-Arrhenius model of thermal activation, and are instead indicative of cooperative aging of the antiferromagnet. Our results provide new insights into the mechanisms controlling the stationary states and dynamics of ferromagnet/antiferromagnet bilayers, and potentially other frustrated magnetic systems.

I. INTRODUCTION

Aging is a spontaneous evolution of the system's properties under fixed experimental conditions, as it relaxes toward equilibrium. It entails a decrease of the free energy and a slow change of thermodynamic averages.[1] In the simplest case of a classical two-state system trapped in a metastable state, the probability that it relaxes into the equilibrium state is exponentially dependent on time, with the characteristic time constant described by the Arrhenius equation [see Sec. IV]. Aging is also common to frustrated systems, where significant deviations from the Arrhenius law are generally observed. The aging characteristics of frustrated systems are determined by their complex potential landscape, and provide insight into a number of important properties such as the nature of the equilibrium state, the relevant degrees of freedom, and the susceptibility to external perturbations. In amorphous materials with quenched disorder,[2–4] measurable quantities such as the thermo-remanent magnetization[5] and the thermal energy[6,7] decrease intermittently. However, even simple coarsening systems can exhibit an aging phenomenology that evolves gradually.[8] In granular systems, the total energy has been observed to decay inverse-logarithmically,[9] or exhibit a weak power-law[10] relaxation towards saturation in the ground state.

In magnetic systems, aging has been extensively explored in diluted spin glasses, where frustration arises due to the random variations of long-range exchange interactions in the bulk of the material.[11] However, surprisingly little is known about the aging effects in frustrated magnetic thin-film heterostructures that play an important role in modern information technology. A proverbial example of such a system is a ferromagnet/antiferromagnet (F/AF) bilayer. The most well-known phenomenon exhibited by F/AF bilayers is exchange bias (EB) - asymmetry of the magnetic hysteresis loop acquired by F below the Neel temperature T_N of AF,[12] which is utilized in magnetic sensors, e.g. in computer hard drives, to "pin" the magnetization of F. The EB effects are two orders of magnitude weaker than the local exchange interaction across the F/AF interface. However, the latter is generally randomized due to the unavoidable interface roughness and/or atomic-scale intermixing of the interface, resulting in only small residual average effects. Nevertheless, both F and AF in a F/AF bilayer experience a large local random exchange field that varies on the atomic length scale and can lead to magnetic frustration.

The F/AF system can be a fertile ground for the studies of frustration effects, since its properties can be easily controlled by the experimental parameters. For example, the average magnitude of the effective random field is inversely proportional to the thickness of the corresponding magnetic layer, and therefore can be independently varied for both F and AF by the appropriate choice of the film geometry. Random field exerted by AF on F should vanish above T_N, and gradually increase with decreasing temperature $T < T_N$. Converse is also true for the effects of F on AF with respect to the Curie temperature T_C of F. The external field H stabilizes the ferromagnetic order but has a negligible effect on AF ordering. Thus, by varying H and T, one can explore the effects of competition between ordering and disordering contributions to the state of the system over a broad range of parameters, in an experiment performed on a single system, thus eliminating the obscuring effects of statistical variations. Furthermore, one can explore the effects of spin dimensionality by studying magnetic materials with different internal magnetic anisotropies, which can be controlled independently from the random field. One can also explore the effects of spatial dimensionality, for example the crossover from two to three dimensions, by stacking thin-film F/AF bilayers into a thick multilayer.

There is presently little evidence for the frustration

effects in F/AF bilayers. A recent study involving one of us[13] demonstrated aging in a thin-film epitaxial AF $Fe_{50}Mn_{50}$=FeMn, in bilayers with ferromagnetic $Ni_{80}Fe_{20}$=Permalloy=Py. Measurements of the dependence on the magnetic history and temperature provided evidence for the non-Arrhenius nature of relaxation, consistent with the expected effects of frustration. However, it is not known whether the observed effects are specific to the studied epitaxial system or generic to F/AF bilayers that are typically polycrystalline. In contrast to the single-crystalline systems, interactions among AF grains are often expected to be negligible for polycrystalline systems, and as a result simple Arrhenius-type relaxation is predicted for such systems.[14–16] It is also not known if frustration can be controlled by varying the thickness of the magnetic films, as suggested above.

Here, we demonstrate non-Arrhenius aging in bilayers of a polycrystalline antiferomagnet CoO with ferromagnetic Py. In contrast to the previously studied FeMn-based bilayers, the Neel temperature of CoO $T_N = 290$ K is readily experimentally accessible, enabling measurements of aging for different AF thicknesses throughout the entire temperature range relevant to the magnetic ordering in CoO. We show that the aging characteristics of thin polycrystalline CoO are remarkably similar to those of thin epitaxial FeMn, suggesting that the observed behaviors are generic to thin-film F/AF bilayers, regardless of crystallinity and specific material properties. With increasing CoO thicknesses, we first observe a decrease of aging at low temperatures, and for even thicker films a complete disappearance of aging at any temperature. These behaviors are qualitatively consistent with the higher activation energy barriers expected for the Arrhenius-type activation. However, measurements of the dependence on temperature and aging history show that aging is cooperative and cannot be described by the Neel-Arrhenius model, providing further evidence for the significance of frustration effects in this system.

The paper is organized as follows. In the next section, we present experimental measurements of aging in CoO, including its dependence on thickness, magnetic history and temperature. The two main purposes of the presented experiments are i) to establish the general features of aging in F/AF bilayers, and ii) to demonstrate that the Neel-Arrhenius activation model is not applicable to these systems. In Sec. III, we present simulations of aging based on a simple two-dimensional Ising model that capture the salient experimental features. Section IV summarizes our observations and analysis. Section IV establishes the relation between the time-dependent magnetoelectronic signals utilized in our measurements and the evolution of magnetization. Sec. IV presents analysis of aging expected for systems described by the Neel-Arrhenius model.

II. EXPERIMENT

The samples utilized in our study were fabricated by magnetron sputtering at room temperature, in a high-vacuum deposition chamber with the base pressure of less than 1×10^{-8} Torr. First, a CoO layer with thickness d was deposited by reactive sputtering in a mixture of Ar and O_2, followed by the deposition of a 10 nm thick Py layer in ultrapure Ar, and finally a 20 nm thick capping SiO_2 layer protecting the structure from oxidation. The deposition rates for all the layers were between 0.3 and 0.5 A/s. The roughness of the surfaces/interfaces of about 0.3 nm rms, similar to the substrate surface roughness, was determined by atomic force microscopy using samples whose deposition was stopped at the corresponding stages of the process. The partial pressure of O_2 required to achieve stoichiometric CoO was optimized using a series of test CoO/Py samples, as described in Ref. [17]. The films deposited in excess oxygen pressure exhibited a reduced Neel temperature T_N, and a rapid increase of exchange bias (EB) at temperatures below 50 K associated with the freezing of 'loose' oxygen spins.[18] Similarly, under-oxidized CoO films exhibited reduced EB. Optimized properties were achieved at partial oxygen pressure of about 2×10^{-5} Torr.

We studied six samples with CoO thickness $d = 2$, 4, and 10 nm, labeled CoO2, CoO4, and CoO10 respectively, with results verified for each thickness in two nominally identical samples. Their magnetic properties such as the blocking temperature T_B characterizing the onset of the hysteresis loop asymmetry - the exchange bias (EB) - were consistent with the previous measurements of EB in thin polycrystalline CoO films.[19] The characterization and studies of aging were performed using magnetoelectronic measurements in the four-probe van der Pauw geometry, with ac current $I = 0.1$ mA rms at a frequency $f = 1.3$ kHz, and lock-in detection of ac voltage V. At a fixed temperature, the variations of resistance R were caused by the anisotropic magnetoresistance (AMR) of Py. To obtain a well-defined initial magnetization state of both F and AF, in all of the measurements described below, the samples were cooled starting from $T = 300K$ above the Neel temperature $T_N = 290$ K of CoO at a rate of 4 K per minute, in a saturating field $H = 500$ Oe. In all the measurements, the field was applied in-plane perpendicular to the average direction of current, resulting in a minimum of AMR when the magnetization M of Py was aligned with the field.

Figure 1(a) shows a representative magnetoelectronic hysteresis loop for the CoO2 sample acquired at $T = 5$ K. The dependence of R on H reflects the field-dependent orientation of the Py magnetization, resulting in a variation of the anisotropic magnetoresistance $R(\theta) = R_{min} + \Delta R sin^2(\theta)$, where θ is the angle formed by the local direction of M relative to the direction of H, R_{min} is the minimum of resistance at $\theta = 0$, which is approached at large H, and ΔR is the magnetoresistance. The peaks at fields H_+ and H_- are identified with the reversal of

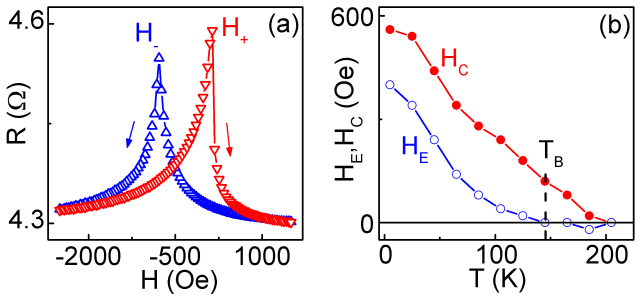

Figure 1. Magnetic properties of the CoO2 sample. (a) Magnetoelectronic hysteresis loop obtained at 5 K after two prior similar "training" loops, (b) Temperature dependence of coercivity H_C and exchange bias field H_E.

M. The corresponding peak values of resistance are close to the resistance maximum $R = R_{min} + \Delta R = 4.66\ \Omega$ at 5 K, implying that the reversal occurs through the magnetization orientation almost uniformly orthogonal to H. This result is surprising, given the expected large random variations of exchange interaction at the F/AF interface, but is consistent with the previous observations for epitaxial FeMn/Py bilayers.[13]

The hysteresis loop becomes asymmetric below the blocking temperature $T_B = 145$ K. This asymmetry is quantified by the effective EB field $H_E = (H_+ + H_-)/2$ that increases with decreasing $T < T_B$ [Fig. 1(b)]. The coercivity $H_c = (H_+ - H_-)/2$ characterizing the broadening of the hysteresis loop also increases with decreasing $T < T_B$. These thickness- and temperature-dependent magnetic properties are consistent with the previous measurements of EB for thin polycrystalline CoO films.[19]

To observe aging, the field H was reversed from the initial value H_i below H_- to the final value H_f above H_+, and resistance was recorded in 1 s time steps while keeping all the experimental parameters constant. In the experiments described below, both the time Δt_i of "pre-aging" at field H_i and the aging time at field H_f were 1000 s, unless specified otherwise. When multiple aging experiments were performed, the field was reversed to H_i immediately after completing the aging measurement, and the above procedure was repeated. In all the measurements, the field was ramped at a fixed rate of 2 kOe/s. The value of H_f was chosen so that the corresponding value of R was larger than R_{min} by approximately $0.1 - 0.3$ of the full MR. The corresponding average angle formed be the Py magnetization M with respect to the direction of the field was $\theta \approx 18 - 33°$. At these relatively small angles, the variation of the magnetoelectronic signals is to a good approximation proportional to the variation of the effective exchange field exerted by CoO on Py, as shown in Sec. IV. Thus, the evolution of the magnetoelectronic signals is a direct quantitative measure of the aging dynamics in CoO.

Figure 2(a) shows several aging curves for CoO2 squentially acquired after field-cooling. We obtained a good

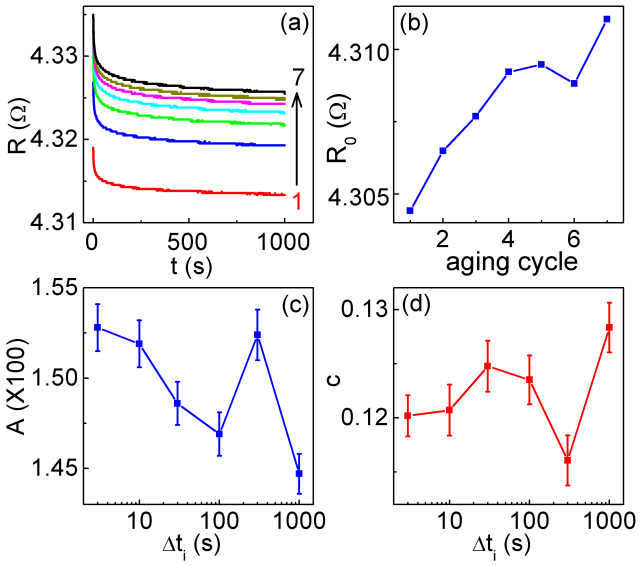

Figure 2. Aging in the CoO2 sample at $T = 5$ K obtained at field $H_f = 400$ Oe, after pre-aging at field $H_i = -1600$ Oe. (a) Aging dependencies were obtained sequentially, as labeled, immediately after cooling from $T = 300$ K in field $H = 500$ Oe. Each measurement was preceded by aging over time $\Delta t_i = 1000$ s at field $H_i = -1600$ Oe. (b) Asymptotic resistance extracted from the power-law fitting of data in panel (a) vs the number of the aging cycle. The fitting uncertainty is similar to the symbol size, (c,d) relaxation scale A (c) and power-law exponent (d) extracted from the power-law fitting of aging data obtained with different pre-aging times $\Delta t_i = 1000$ s, 300 s, 100 s, 30 s, 10 s, and 3 s. The values of R_{min} and ΔR at 5 K are 4.29 Ω and 0.38 Ω, respectively.

fitting to all the aging data by using a power-law dependence $R = R_0 + At^{-c}$. An alternative fitting with an inverse logarithmic dependence also produced a good fit, but the uncertainty of the fitting parameters was generally more significant. We use power-law fitting in the analysis described below. The main difference among the sequential aging curves is the overall upward shift of resistance, as illustrated by the monotonic increase of R_0 extracted from the power-law fitting [Fig. 2(b)]. Both the scale A and the power-law exponent c exhibited only small random variations [not shown]. The dependence of aging characteristics on the prior aging history is in a quantitative agreement with the previous measurements of epitaxial FeMn,[13] suggesting that these are robust characteristics reflecting the general aging mechanisms in the F/AF bilayers. We note that the dependence of R_0 on the aging history is inconsistent with the Neel-Arrhenius activation model, which predicts relaxation towards a unique equilibrium state characterized by $R = R_{min} = 4.29\ \Omega$ for the CoO2 sample at 5 K, independent of the previous aging history.

We performed several additional tests for the applicability of the Arrhenius model, as described below. In one of the tests, the "pre-aging" time Δt_i in the reversed state

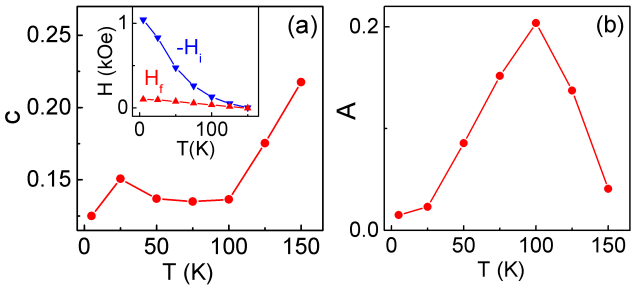

Figure 3. The power-law exponent c (a) and the scale A (b) vs T, for the CoO2 sample. Inset in (a) shows the temperature-dependent values of H_f and $-H_i$ used in these measurements. The values of R_{min} and ΔR are: 4.29 Ω, 0.38 Ω at 5 K; 4.31 Ω, 0.38 Ω at 25 K; 4.35 Ω, 0.39 Ω at 50 K; 4.52 Ω, 0.39 Ω at 75 K; 4.67 Ω, 0.39 Ω at 100 K; 4.82 Ω, 0.38 Ω at 125 K; 4.98 Ω, 0.365 Ω at 150 K.

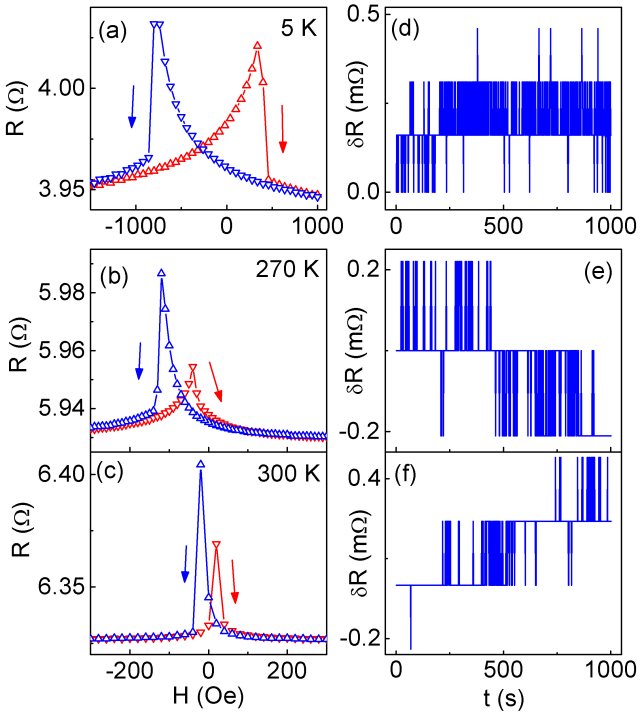

Figure 4. (a-c) Magnetoelectronic hysteresis loops, and (d-f) aging data for the CoO10 sample. The values of H_i, H_f used in aging measurements were: −830 Oe and 430 Oe in (d), −130 Oe and −20 Oe in (e), −30 Oe and 30 in (f), respectively. The hysteresis loops were acquired after 2 prior "training" loops, and δR is the resistance variation relative to the first acquired value. The values of R_{min} and ΔR are: 3.93 Ω, 0.38 Ω at 5 K; 5.92 Ω, 0.30 Ω at 270 K; 6.32 Ω, 0.29 Ω at 300 K, respectively.

was varied. According to the Neel-Arrhenius model, most of the grains with long activation times τ do not become activated for short $\Delta t_i \ll \tau$, resulting in smaller aging effects at long times. The corresponding analytical expression derived in Sec. IV generally deviates from the power-law form, but for very short Δt_i it can be approximated as a power law with exponent $(c+1)$. The results of measurements performed with Δt_i varied from 3 s to 1000 s are presented in Fig. 2(c,d). Both the exponent c and the scale A obtained from the power-law fitting exhibit only small random variations inconsistent with the Neel-Arrhenius model. Similar results were obtained for the epitaxial FeMn-based bilayers.[13] This implies that the magnetic grains, or more generally the subsystems that become activated during the aging process, strongly interact with each other, resulting in cooperative activation not described by the Neel-Arrhenius model.

The dependence of the aging characteristics on temperature provides further insight into the aging mechanisms. We observed aging in the CoO2 sample starting from the lowest measured temperature of 5 K to above the blocking temperature $T_B = 145$ K. At each measurement temperature, the aging field H_f was adjusted so that the corresponding value of R was above the AMR minimum R_{min} by about 1/3 of the total AMR, as discussed above. For a system characterized by the power-law aging at some temperature T_0, the Neel-Arrhenius model predicts that the power-law exponent varies as $c(T) = c(T_0) + \ln(T/T_0)$, see Sec. IV. The experimentally determined exponent $c(T)$ exhibits a much smaller increase from $c = 0.125$ at 5 K to 0.21 at 150 K [Fig. 3(a)]. A similar small increase from approximately $c = 0.1$ at 5 K to 0.2 at 200 K was previously observed for expitaxial FeMn.[13]. The aging scale A exhibits a sharp peak at 100 K. Its decrease at lower temperatures can be qualitatively attributed to "freezing out" of AF spins. As temperature increases above 100 K, the potential landscape of AF likely becomes so shallow that there are very few metastable states with relaxation times long enough for our measurements. This temperature dependence of A is different from FeMn, where only a decrease of A at high-temperature was observed. The difference between the two systems likely originates from the stronger temperature dependence of magnetocrystalline anisotropy of CoO, compared to FeMn.

In addition to the dependence on temperature and magnetic history, the thickness of the magnetic film is expected to affect aging. In the framework of the granular model, the grain volume is expected to be proportional to the thickness of the film, accordingly modifying the activation energy. At a given temperature, the characteristic activation times should increase with increasing thickness of AF. Since the activation time is determined by the ratio of the activation energy to temperature, this implies that aging in thicker films should be observed at higher characteristic temperatures, approaching the Neel temperature T_N for large AF thicknesses. In particular, if aging is observed above 5 K for a 2 nm thick film, then for a 10 nm thick film it can be expected above 25 K. Measurements of temperature- and thickness-dependent aging effects for CoO are facilitated by the easy experimental accessibility of its $T_N = 290$ K. We have performed

measurements similar to those described above for two additional thicknesses of CoO, 4 nm (sample CoO4) and 10 nm (sample CoO10). We first describe the results for CoO10, which exhibits behaviors starkly different from CoO2, and then discuss the intermediate case of CoO4.

For the Co10 sample, we performed measurements of the hysteresis loops and aging at temperatures ranging from 5 K to 300 K, above T_N. Representative results for $T = 5$ K, 270 K, and 300 K are shown in Fig. 4. Three features qualitatively distinguish the hysteresis loops for CoO10 from those for CoO2. First, the variation of resistance is only about 10% of the total magnetoresistance. Second, the resistance abruptly drops after reaching the peak, instead of gradually decreasing with increasing magnitude of H. Finally, there is negligible hysteresis of resistance after the drop. These observations indicate that the magnetization of Py abruptly reverses through a highly inhomogeneous state via an avalanche. The closing of the hysteresis loop right after the reversal provides evidence for the absence of aging, which is confirmed by direct measurements shown in Figs. 4(d-f). Aside from the digitization steps, the variations in these data do not exceed 0.2% of the total AMR, and are likely caused by the slight temperature drift. The lack of aging at any temperature relevant to magnetism in CoO is inconsistent with the granular activation picture, according to which one would expect aging to appear for thick CoO at temperatures close to T_N. Instead, it is likely that small effects of exchange interaction with Py scaling inversely with the AF thickness are insufficient to disturb the magnetization state of CoO. It is presently not clear how this observation can be reconciled with the existence of EB in this system, which implies that the exchange interaction with Py is sufficiently strong to perturb the magnetization state of CoO. One possibility is that the effects of aging in CoO on Py very close to T_N are simply too small for detection with our technique.

The behaviors of the CoO4 sample with a 4 nm CoO layer are intermediate between those of CoO2 and CoO10. At low temperatures, the hysteresis loop exhibits a sharp drop of resistance at the reversal points, and variations of resistance that constitute only a small fraction of the total AMR [Fig. 5(a)]. The resistance variations become gradual and approach the total AMR at higher temperatures [Fig. 5(b)]. The low-temperature characteristics closely match those of the CoO10 sample, while at higher temperatures they are similar to CoO2. These similarities are confirmed by the measurements of aging, which demonstrate negligible variations of resistance at low temperatures, and significant aging at higher temperatures [Fig. 5(c)]. Power-law dependence provided a good fit to the aging data over the entire of temperature between $T = 190$ K and $250K$ K, where significant aging was observed. With increasing temperature, the scale A increases to a peak at $T = 225$ K, and then decreases again at higher T, while the exponent c increases from about 0.1 at 200 K to about 0.4 at $T = 240$ K.

We note that the temperature dependence of aging

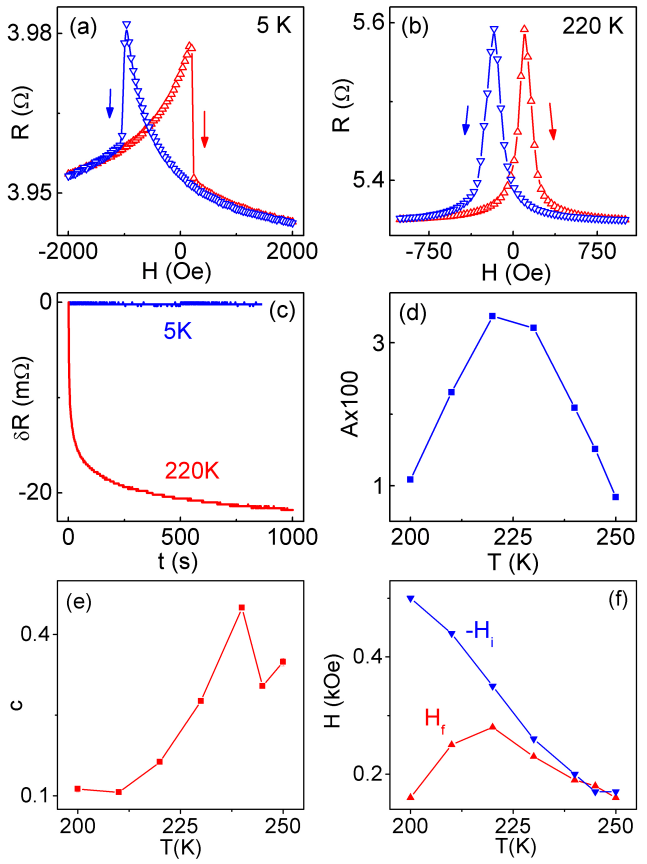

Figure 5. Results for the CoO4 sample. (a,b) Magnetoelectronic hysteresis loop obtained at $T = 5$ K (a) and 220 K (b), after 2 prior similar loops. (c) Aging data obtained at 5 K and 220 K, as labeled. δR is the resistance variation relative to the first acquired value, (d,e) relaxation scale A (d) and Power-law exponent c (e) vs T, (f) Temperature dependence of $-H_i$ and H_f used in the measurements of aging. Aging data at 5 K were obtained at field $H_f = 240$ Oe, after preaging at field $H_i = -1020$ Oe. The values of R_{min} and ΔR are: 3.94 Ω and 0.38 Ω at 5 K, 5.07 Ω, 0.34 Ω at 200 K; 5.21 Ω, 0.335 Ω at 210 K; 5.30 Ω, 0.33 Ω at 220 K; 5.46 Ω, 0.325 Ω at 230 K; 5.60 Ω, 0.32 Ω at 240 K; 5.66 Ω, 0.32 Ω at 245 K; 5.73Ω, 0.315 Ω at 250 K.

in the CoO4 sample is at least qualitatively consistent with the granular activation model. The absence of aging at low temperature can be interpreted in terms of the freeze out of all the grains, while the reduction of aging effects at $T > 225$ K can be indicative of fast activation that cannot contribute to our slow aging measurements. The variation of the exponent c is also in a semi-quantitative agreement with the Neel-Arrhenius model, [see Sec. IV]: for $c(T = 200K) = 0.1$, the model predicts $c(T = 240K) = 0.1 + \ln(1.15) = 0.3$, not far from the experimental value.

Based on the observed hysteresis and aging for different CoO thickness, one can make a general conclusion important for the interpretation of magnetic hysteresis loops in F/AF bilayers and perhaps other frustrated magnetic

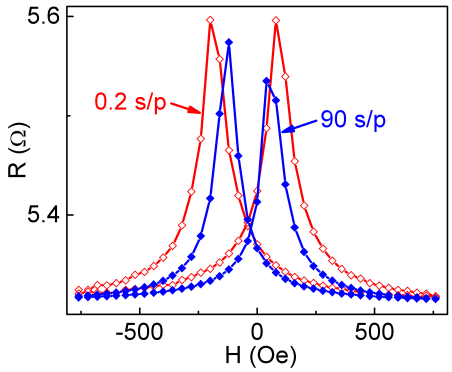

Figure 6. Two hysteresis loops for the CoO4 sample acquired at the same $T = 220$ K, after several similar training loops. Data were acquired at a rate of 0.2 s/point (open symbols) and 90 s/point (solid symbols).

systems. Namely, abrupt reversal followed by the closing of the hysteresis loop is observed in the absence of aging. Significant aging effects are correlated with gradual magnetization rotation through a configuration in which the magnetization is almost uniformly perpendicular to the field. In this case, the observed gradual closing of the hysteresis loop after reversal is consistent with the presence of aging effects concurrent with the field sweep during the hysteresis measurement. We have verified this conclusion by performing hysteresis loop measurements at different field ramp rates, as illustrated in Fig. 6. Slower rates result in a smaller hysteresis, as expected for the aging effects. Both the coercivity and the EB field extracted from the two sweeps differ by about a factor of two, demonstrating that these characteristics are not well defined for F/AF systems that exhibit aging.

III. SIMULATIONS OF AGING BASED ON THE 2D RANDOM FIELD ISING MODEL

The preceding Sec. II presented evidence for the cooperative nature of aging phenomena in thin-film F/AF bilayers, which generally cannot be described by the Neel-Arrhenius activation model. In this Section, we introduce a simple model that captures the salient features of aging observed in our measurements, providing insight into the aging mechanisms. Our analysis is based on the random-field Ising model (RFIM),[20,21] which has been extensively utilized for modeling diluted antiferromagnets,[22] impure substrates ,[23] and magnetic alloys.[24] We make several simplifying approximations. First, we are interested only in the aging phenomena in AF, and therefore restrict the model to this layer. We assume that the magnetization state of the thin AF film does not vary through its thickness, so that it can be approximated by a two-dimensional (2d) square spin lattice. We consider the staggered AF order parameter, which is modeled by the ferromagnetic exchange interaction of each spin with its

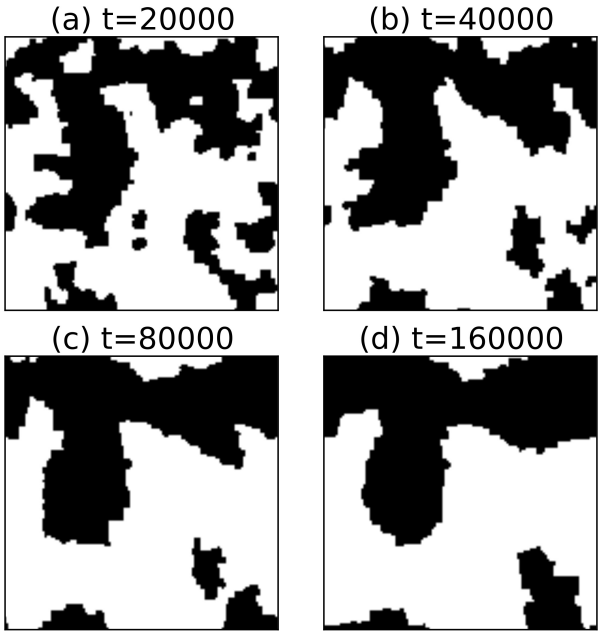

Figure 7. Spin pattern snapshots in the Monte Carlo simulation at $T = 0.3$ for the system size $L = 128$, with random field flipped after every 20000 sweeps. (a) After annealing, just before the first random field flip, (b) at the end of the first aging cycle, just before the second random field flip, (c) just before the fourth random field flip, (d) just before the eighth random field flip.

four nearest neighbors. The dipolar spin-spin interactions and the interaction with the modest external fields used in our experiments are negligible. The exchange interaction with F layer is described by an uncorrelated quenched random field h with a Gaussian distribution $\mathcal{N}(0, \sigma^2_{\rm rand})$ of zero mean and width $\sigma_{\rm rand}$. In this approximation, the reversal of the magnetization of F utilized in our experiments to initiate aging is modeled by the reversal of the random field. The Hamiltonian for this model is

$$\mathcal{H} = -J \sum_{<i,j>} s_i s_j - \sum_{i=1}^{N=L^2} h_i s_i \qquad (1)$$

where the coupling constant J sets the overall energy scale and is set to 1 here. The spins are bimodal in the Ising limit, $s_i = \pm 1$, where $< i, j >$ enumerate nearest-neighbor spins, L is the linear dimension of the 2D square lattice with the total number of spins $N = L^2$ and periodic boundary conditions. The effects of temperature are modeled by the sequential random flipping of spins with the probability $P = \exp(-\Delta E/T)$, where ΔE is the energy change upon spin flip. Time t is measured in sweeps, where one sweep corresponds to N random sequential update attempts. Temperature T is measured in units of J.

A wide range of values was explored for each simulation parameter. For example, we varied the random

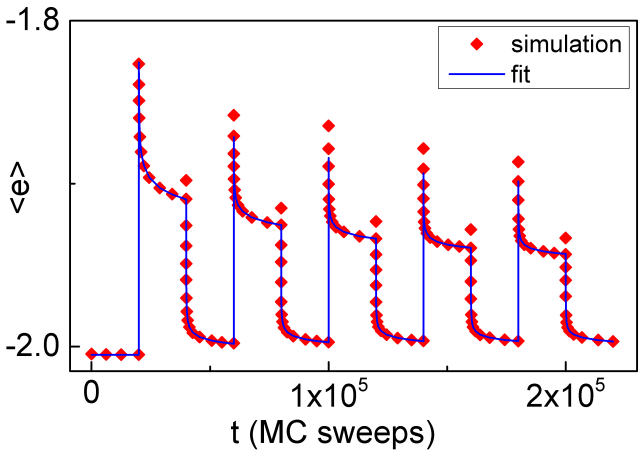

Figure 8. Average energy per spin vs time, for the system size $L = 128$, random field $\sigma_{\rm rand} = 1.0$, at temperature $T = 0.3$ after quasi-adiabatic annealing. The random field is flipped every 20000 sweeps. Symbols: simulation, curves: power-law fits with Eq. (2).

field $\sigma_{\rm rand}$ from 0.1 to 2.0, and found that significant aging effects appeared only at $\sigma_{\rm rand}$ approaching $J(= 1)$. This result is somewhat surprising, given that the effective random fields caused by exchange interaction at the F/AF interface should become comparable to internal exchange only for film thickness approaching a single atom. We leave this issue to future more realistic analyses.

To simulate the slow field-cooling, we anneal the system quasi-adiabatically starting from $T_{n=0} \gg 1$, with the temperature during the n-th sweep $T_n = 0.9999T_{n-1}$. After the annealing, the system reaches a metastable state with interlocking spin domains of oppositely oriented spins [Fig. 7(a)]. While almost all spins are aligned with their neighbors at the end of annealing and attain their Ising-energy per spin, $\langle e\rangle \approx -2$ [see Fig. 8], a subextensive amount of energy remains stored in rough domain walls that are pinned by the random field. To initiate aging at a fixed temperature T, we flip the random field and simulate the evolution over 20,000 sweeps, after which the random field is flipped again and the simulations are repeated. The field flip brings the system into an unstable state, dislodging the domain walls. The snapshots of the spin distributions taken in the end of different aging cycles in Fig. 7 show evolving spatial patterns, indicating that the system does not relax to a unique equilibrium state, consistent with our experimental result Fig. 2.

To compare the results of our simulations to the experimental observations, we analyzed the evolution of the average energy per spin $\langle e\rangle$. We argue that the functional form of the time dependence of $\langle e\rangle$ is likely the same as that of the measured magnetoresistance, since the latter is directly proportional to the Zeeman energy of the ferromagnet, and other contributions to the energy of the F/AF system may be expected to evolve in a similar manner. An example of the time dependence of $\langle e\rangle$ including ten sequential aging cycles, starting from an annealed state, is shown in Fig. 8. The obtained dependencies can be well described by the power-law

$$e(t) = e_0 + At^{-c} \qquad (2)$$

where e_0 is the asymptotic (equilibrium) energy, A and c are the scale and the exponent, respectively, and time t is measured in the units of the Monte Carlo sweep. We note that changing the time scale in Eq. 2 simply rescales the value of A without any effect on the exponent c, allowing direct comparison of the latter with the experiment.

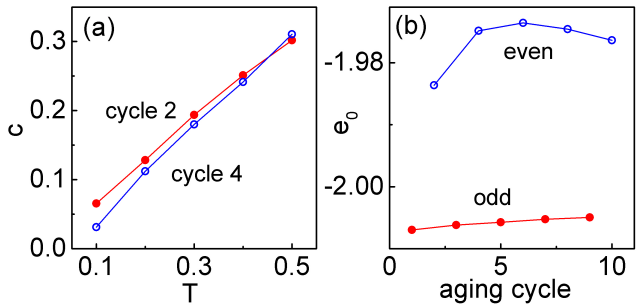

Figure 9. Power-law fitting of simulations for the system size $L = 128$ with random field $\sigma_{\rm rand} = 1.0$. (a) Dependence of exponent c on temperature, for two representative cycles. (b) Asymptotic energy e_0 for different aging cycles. The quantities in both panels are defined by Eq. 2.

Figure 9(a) shows the dependence of the power-law exponent c determined from the simulations on temperature for two aging cycles. The characteristic values of c do not significantly depend on the aging cycle number, and are very close to those obtained in our experiments. The simulations also reproduce the relatively slow increase of c with increasing temperature. This result is inconsistent with the Neel-Arrhenius model. For example, for $c \approx 0.05$ at $T = 0.1$, this model would predict $c = 1.7$ at $T = 0.5$, a much larger increase than in Figure 9(a). There is no aging on any meaningful timescale at $T = 0$, as expected for thermal relaxation of the system. Figure 9(b) shows the dependence of the asymptotic energy value e_0 on the cycle number. The evolution of e_0 provides further evidence that the system does not relax to a unique equilibrium state, and thus cannot be described by the Neel-Arrhenius model.

IV. SUMMARY AND CONCLUSIONS

To summarize our experimental findings, we observed and analyzed significant aging effects in thin-film polycrystalline CoO/Permalloy bilayers. The aging characteristics depend on the parameters such as the thickness of CoO, temperature, and magnetic history. In all cases, aging is well approximated by the power law with a subunity exponent. For 2 nm thick CoO, aging is observed

over a wide range of temperatures and its characteristics are remarkably similar to those previously observed in 2 nm thick $Fe_{50}Mn_{50}$, suggesting that the observed behaviors are generic to F/AF bilayers. No aging is observed for a 10 nm thick CoO film at any temperature. For the 4 nm thick CoO film, aging is observed in a relatively narrow range of temperatures between 190 and 250 K. Our measurements revealed a correlation between the magnetic hysteresis loop and aging, which provides a simple test for the presence of aging in other F/AF systems, and demonstrates that the coercivity and exchange bias, commonly used to characterize the hysteresis loop of F/AF bilayers, are not well defined in the presence of aging.

To gain insight into the mechanisms of aging, we studied the dependence of aging characteristics in the 2 nm thick CoO film on its magnetic history. These measurements revealed large inconsistencies with the Neel-Arrhenius model commonly applied to polycrystalline thin-film F/AF systems. First, the experimentally determined asymptotic value of resistance during the aging process significantly depends on the magnetic history, while the Neel-Arrhenius model predicts that the system asymptotically reached the ground state, independently of history. Second, the power-law exponent characterizing aging is independent of the duration of aging in the state with reversed magnetization of F, while the Neel-Arrhenius model predicts reduced aging at long times approximately described by a larger power-law exponent. The experimental dependence of the exponent on temperature is significantly smaller than expected from the Neel-Arrhenius model. The complete absence of aging in the 10 nm thick CoO is also likely inconsistent with the Neel-Arrhenius model, which predicts a gradual increase of the characteristic activation temperature with increasing film thickness.

We have developed a simple alternative model that incorporates only two contributions to the energy of the AF film: the nearest-neighbor exchange interaction between AF spins, and the effective random field produced by the exchange interaction with F. Our model reproduces the power-law aging and some of the other salient experimental features. The agreement provides a strong evidence for the dominance of frustration caused by the random exchange interaction at the F/AF interface.

ACKNOWLEDGEMEMTS

This work was supported in part by the NSF grants DMR-1207431 and DMR-1504449.

APPENDIX A: RELATIONSHIP BETWEEN MAGNETOELECTRONIC MEASUREMENTS AND MAGNETIZATION AGING

The evolution of the magnetoelectronic signals, due to the anisotropic magnetoresistance (AMR), is caused by the temporal evolution of the angle θ formed by the local magnetization M of F relative to the electrical current. In our experiment, the latter is aligned perpendicular to the external field H, such that the resistance minimum is achieved at $\theta = 0$. The magnetic anisotropy of the ferromagnet (Permalloy) is negligible on the scale of the fields applied in our experiments, so the finite value of θ can be attributed entirely to the exchange interaction with AF. This interaction can be modeled by the time-dependent and spatially varying effective exchange field H' with components $H'_{\parallel}$, $H'_{\perp}$ that are parallel and perpendicular to the applied field, respectively. In terms of these components, the angle θ is defined by

$$\tan(\theta) = \frac{H'_{\perp}}{H'_{\parallel} + H}, \tag{3}$$

and the measured resistance is

$$R = R_{min} + (R_{max} - R_{min})\ \frac{1 - cos(2\theta)}{2}, \tag{4}$$

where R_{min} (R_{max}) is the minimum (maximum) of AMR. The aging experiments are performed at relatively large H, such that the resistance value is approximately $0.1 - 0.3$ of the total MR above R_{min}, corresponding to relatively small average $\theta \approx 18 - 33°$. For these values of θ, $H' \lesssim$, and the second-order expansion

$$R(\theta) \approx R_{min} + (R_{max} - R_{min})\theta^2 \tag{5}$$

gives an error of less than 8%. To establish the relationship between the time-dependent resistance and aging of AF, we note that the observed variations of R due to aging are much smaller than the total AMR, i.e., $\Delta\theta \ll \theta$, where $\Delta\theta$ is the variation of θ due to aging. According to Eq. (5), the corresponding variation of resistance is

$$R(\theta + \Delta\theta) = R_{min} + (R_{max} - R_{min})(\theta + \Delta\theta)^2, \tag{6}$$

$$\approx R(\theta) + 2\theta(R_{max} - R_{min})\Delta\theta, \tag{7}$$

i.e. the observed small variations of R are linear in $\Delta\theta$. Similarly expanding Eq. (3) in terms of the small variations of the effective exchange field $\Delta H'_{\parallel}$, $\Delta H'_{\perp}$ caused by aging, we obtain $\Delta R \propto \Delta H'_{\perp}$. The variations of the latter are a direct measure of the evolution of the staggered magnetization of AF, as described e.g. in the Neel-Arrhenius model by Eq. (10). Thus, our magnetoelectronic measurements can be interpreted, up to a scaling parameter, directly in terms of the AF aging dynamics, without the need for any technique-dependent corrections of the measured functional dependence.

APPENDIX B: NEEL-ARRHENIUS MODEL OF AGING

According to the Arrhenius law,[25] the characteristic time it takes for a particle to remain trapped in a metastable state in a potential well is

$$\tau = \tau_0 \exp\left\{\frac{U}{k_B T}\right\}, \tag{8}$$

where τ_0 is the attempt time determined by the dynamics of the particle in the potential well, U is the activation barrier, k_B is the Boltzmann constant, and T is the temperature of the thermal bath. Accordingly, the probability that the particle initially trapped in the well remains trapped at time t is

$$P(t) = e^{-t/\tau}. \tag{9}$$

The Neel-Arrhenius model describes the magnetization reversal in granular magnetic materials in terms of the Arrhenius law, which is applied to individual magnetic grains. The activation barrier U for each grain depends on its magnetic anisotropy, volume, and magnetization (for ferromagnets), as described by the Neel-Brown model.[26] In the trivial case when all the grains are identical, one expects exponential relaxation of the magnetization towards its equilibrium state, as follows from Eq. 9 applied to a statistically large number of subsystems, $M(t) - M(\infty) = [M(0) - M(\infty)]e^{-t/\tau}$. The initial metastable state is prepared, for example, by suddenly changing the magnitude and/or direction of the applied magnetic field H. More generally, the magnetic grains can vary in size, magnitude and orientation of their anisotropy. Defining $\rho(\tau)$ as the relative volume density of grains with activation time τ, we obtain

$$M(t) - M(\infty) = [M(0) - M(\infty)] \int e^{-t/\tau}\rho(\tau)d\tau. \tag{10}$$

This relationship can be in principle expected not only for the ferromagnetic (F), but also for the antiferromagnetic (AF) grains, with M interpreted as the staggered magnetization. In practice, the distribution of grains is usually not known. Furthermore, the magnetic materials described by this model may not be formed by the well-defined isolated grains. An important question is then whether one can infer the grain distribution, and more generally the applicability of the model, from the measured magnetization aging curve $M(t)$. To answer this question, we note that by introducing a new variable, the rate $r = 1/\tau$, Eq.(10) is transformed into

$$M(t) - M(\infty) = -[M(0) - M(\infty)] \int e^{-tr}\rho(r)dr/r^2. \tag{11}$$

Since $[M(t) - M(\infty)]$ is a (reversible) Laplace transform of $\rho(r)/r^2$, one can at least formally find a function $\rho(r)$ that can be interpreted as the distribution of magnetic grains responsible for the observed aging behaviors, regardless of the specific form of $M(t)$. Thus, to determine whether this physical picture is applicable to the studied system, one must develop specific tests, as described below.

1. Grain distribution for power-law aging

Here, we will focus on the specific form of the aging dependence, $R(t) - R(\infty) = At^{-c}$ observed in our experiments. We emphasize the empirical nature of this dependence, which for small c is indistinguishable from the logarithmic dependence $R(t) - R(\infty) = A/ln(t - t_0)$.[9] Aging described by the power law can be modeled in terms of the superposition of contributions from the exponential Arrhenius aging of individual grains,

$$R(t) - R(\infty) = At^{-c} = \Delta R \int_0^\infty \rho(\tau)e^{-\frac{t}{\tau}}d\tau, \tag{12}$$

where ΔR is a normalizing coefficient with the units of resistance proportional to the magnetoresistance of the system, and $\rho(\tau)$ is the relative density of grains with activation time τ. Inverse Laplace transformation then yields

$$\rho(\tau) = \frac{A}{\Gamma(c)\Delta R}\tau^{-(1+c)}, \tag{13}$$

where $\Gamma(c)$ is the gamma function. We note that this distribution cannot be normalized by

$$\int_0^\infty \rho(\tau) = 1, \tag{14}$$

because of the divergence of the integral at small τ for any $c > 0$. This problem can be resolved by introducing a cut-off τ_{min} physically justified by the existence of the smallest grain size present in the system, which cannot be smaller than a single lattice site. The value of τ_{min} affects the normalization constant Δ_R in Eq. 12. Here, we are mainly concerned with the functional form of the aging curves, and therefore below will ignore the subtleties associated with the normalization of the relevant quantities.

2. Dependence on temperature

Assume that at some temperature T, aging exhibits a power-law time dependence characterized by exponent $c(T)$. A Neel-Arrhenius activation model can be then used to analyze the expected aging characteristics at other temperatures. Indeed, one can use Eq. (13) to determine the distribution $\rho_T(\tau)$ of activation times at temperature T, and then Eq. (8) to evaluate the corresponding distribution $\rho_{T'}(\tau)$ at a different temperature T'. In addition to the explicit exponential dependence

on T in Eq. (8), the activation energy U generally decreases with increasing T, and disappears at the Neel temperature T_N of AF. When increasing T, both of these contributions lead to a decrease of τ. At $T \ll T_N$, we can neglect the dependence of U on T, providing a lower bound on the expected variation of τ with temperature. the activation time at T' for a grain characterized by activation time $\tau(T)$ at T is

$$\tau(T') = \tau_0 e^{\frac{U}{kT'}} \approx \tau_0 e^{\frac{U}{kT}(1-\Delta T/T)}, \quad (15)$$

$$= \tau(T)(1 - \Delta T/T)\tau_0^{\Delta T/T}, \quad (16)$$

where we made an approximation $\Delta T = T' - T \ll T$. From Eqs. (15) and (13),

$$\rho_{T'}(\tau) \approx \rho_T(\tau(T)(1 + \Delta T/T)\tau_0^{-\Delta T/T}, \quad (17)$$

$$\propto \tau^{-1-c-\Delta T/T}. \quad (18)$$

The Laplace transform of this expression gives the expected power law exponent for aging at T', $c(T') = c(T) + \Delta T/T$, for small ΔT. Thus, $c(T) = c(T_0) + \ln(T/T_0)$ for arbitrary T, T_0. For example, choosing $T_0 = 5$ K, $T = 200$ K, and using $c(5K) = 0.1$, we get $c(200K) = 3.8$. Such a strong dependence of the power law exponent on temperature is inconsistent with the experimental observations, indicating that the Neel-Arrhenius model is not applicable to this system.

3. Dependence on aging history

The Neel-Arrhenius activation model also makes certain predictions about the dependence of aging behaviors on the previous aging history. In particular, we consider here an experiment that consists of three steps: i) the system is allowed to relax for a very long time with the field applied in a certain direction (defined as '+'), ii) the field is reversed to '-' for a time interval Δt_i, and iii) the aging measurement is performed after again reversing the field to '+'.

We assume that the power-law aging following the form of Eq. (12) is observed for large Δt_i, from which one can infer the distribution Eq. (13) of the grains. After step i) in the aging sequence, all the grains relax to an equilibrium configuration. In step ii), the field is reversed for a time interval Δt_i, resulting in relaxation of only some of the grains. Because of this partial relaxation, only some of the grains become reactivated and can contribute to the subsequent aging in step iii), thus affecting the functional form of aging. To evaluate the relationship between Δt_i and the final aging dependence, we need to account for the probability $P(\tau) = e^{-\Delta t_i/\tau}$ that the grains with the activation time τ were not re-activated during the time interval Δt_i. The grain distribution in Eq. (12) is then replaced by $\rho(\tau)[1 - P(\Delta t_i)]$, yielding

$$R(t) - R(\infty) = \Delta R \int_0^\infty \rho(\tau)[1 - e^{-\Delta t_i/\tau}]e^{-\frac{t}{\tau}}d\tau, \quad (19)$$

$$= A\left[t^{-c} - (t + \Delta t_i)^{-c}\right]. \quad (20)$$

We note that Eq. (19) correctly describes the limiting cases of $\Delta t_i = \infty$ and $\Delta t_i = 0$. In the former case, all the grains should become re-activated during step ii) of the aging sequence. Accordingly, the Δt_i-dependent correction vanishes in this limit, resulting in the expected power law aging dependence. In the latter case, the field has not been reversed at all, so there should be no aging. Indeed, the two terms on the right-side of Eq. (19) cancel each other in this case.

According to Eq. (19), aging at time t comparable to Δt_i cannot be described by the power law. However, since the experimental data could be adequately fit by the power law, we can evaluate the exponent expected for such a fitting from the aging dependence given by Eq. (19). In particular, for very short pre-aging times of a few seconds, most of the aging measurement satisfies $t \gg \Delta t_i$. Expanding $(t + \Delta t_i)^{-1} \approx t^{-c} - c\Delta t_i t^{-(c+1)}$, we obtain

$$R(t) - R(\infty) \approx Ac\Delta t_i t^{-(c+1)}, \quad (21)$$

i.e. one expects to observe a significant increase of the power-law exponent from c to $(c + 1)$. This significant increase of the power law exponent expected from the Neel-Arrhenius model at short Δt_i is inconsistent with the negligible variation of c observed in our experiment.

[1] L.C.E. Struik, *Physical aging in amorphous polymers and other materials,* Elsevier Science Ltd, (1978).
[2] P. Nordblad, P. Svedlindh, L. Lundgren, and L. Sandlund, Phys. Rev. B **33**, 645-648 (1986).
[3] H. Rieger, J. Phys. A **26**, L615-L621, (1993).
[4] P. Sibani and H. Jeldtoft Jensen, EuroPhys. Lett. **69**, 563–569 (2005).
[5] G.G. Kenning, G.F. Rodriguez and R. Orbach, Phys. Rev. Lett. **97**, 057201 (2006).
[6] A. Crisanti and F. Ritort, EuroPhys. Lett. **66**, 253-259 (2004).
[7] P. Sibani, EuroPhys. Jour. B **58**, 483-491 (2007).
[8] G. Biroli, J. Stat. Mech. **5**, P05014 (2005).
[9] E.R. Nowak, J.B. Knight, E. Ben-Naim, H.M. Jaeger, and S.R. Nagel, Phys. Rev. E **57**, 1971-1982 (1998).
[10] D. El Masri, L. Berthier, and L. Cipelletti, Phys. Rev. E **82**, 031503 (2010).
[11] K. Binder and W. Kob, *Glassy Materials and Disordered Solids*, World Scientific, Singapore, (2005).
[12] W.H. Meiklejohn and C.P. Bean, Phys. Rev. **105**, 904 (1956).
[13] S. Urazhdin and U. Danilenko, Phys. Rev. B **92**, 174416 (2015).
[14] E. Fulcomer and S.H. Charap, J. Appl. Phys. **322**, 883 (2010).
[15] M.D. Stiles and R.D. McMichael, Phys. Rev. B **59**, 3722

(1999).
[16] K. O'Grady, L.E. Fernandez-Outon, and G. Vallejo-Fernandez, J. Magn. Magn. Mater. **322**, 883 (2010).
[17] S. Urazhdin, P. Tabor, and W.-L. Lim, Phys. Rev. B **78**, 052403 (2008).
[18] K. Takano, R.H. Kodama, A.E. Berkowitz, W. Cao and G. Thomas, Phys. Rev. Lett. **79**, 1130 (1997).
[19] T. Ambrose and C.L. Chien, J. Appl. Phys. **83**, 6822 (1998).
[20] Y. Imry, S. Ma, Phys. Rev. Lett. **35**, 21 (1975).
[21] T. Nattermann, Spin glasses and random fields, World Scientific **12**, P277 (1997).
[22] J.F. Fernandez, EuroPhys. Lett., **5**, 2 (1988).
[23] J. Villain, J. Phys., **43**, 15 (1982).
[24] D.S. Fisher, G.M. Geoffrey, A. Khurana, Physics Today, **41**, 12 (1988).
[25] S.A. Arrhenius Z. Phys. Chem. **4**, 96-116 (1889).
[26] W.F. Brown, Jr. Phys.Rev. **130**, 1677 (1963).
[27] W. Wernsdorfer, E. Bonet Orozco, K. Hasselbach, A. Benoit, B. Barbara, N. Demoncy, A. Loiseau, H. Pascard, and D. Mailly, Phys. Rev. Lett., **78**, 1791 (1997).
[28] Th. Bauer, P. Lunkenheimer, A. Loidl, Phys. Rev. Lett. **111**, 225702 (2013).